The EMBO Journal vol.9 no.3 pp.663 - 673, 1990

Intermediates of recombination during mating type switching in *Saccharomyces cerevisiae*

C.I.White and J.E.Haber

Rosenstiel Basic Medical Sciences Research Center and Department of Biology, Brandeis University, Waltham, MA 02254, USA

Communicated by F.Stahl

We have identified two novel intermediates of homothallic switching of the yeast mating type gene, from *MAT*a to *MAT*α. Following HO endonuclease cleavage, 5′ to 3′ exonucleolytic digestion is observed distal to the HO cut, creating a 3′-ended single-stranded tail. This recision is more extensive in a *rad52* strain unable to switch. Surprisingly, the proximal side of the HO cut is protected from degradation; this stabilization depends on the presence of the silent copy donor sequences. A second intermediate was identified by a quantitative application of the polymerase chain reaction (PCR). The Yα−*MAT* distal covalent fragment of the switched product appears 30 min prior to the appearance of the *MAT* proximal Yα junction. No covalent joining of *MAT* distal to *HML* distal sequences is detected. We suggested that the *MAT* DNA distal to the HO cut invades the intact donor and is extended by DNA synthesis. This step is prevented in a *rad52* strain. These intermediates are consistent with a model for *MAT* switching in which only the distal side of the HO cut is initially active in strand invasion and transfer of information from the donor.

Key words: recombination mechanisms/mating-type/yeast/double-stranded break/*rad52*

Introduction

In *Saccharomyces cerevisiae* cells expressing the HO gene, *MAT*a cells are induced to switch to *MAT*α, and vice versa, as often as every cell division (reviewed by Nasmyth, 1982; Haber, 1983; Strathern, 1988; Klar, 1989). The switch is a highly efficient mitotic gene conversion event in which ~700 bp of Ya or Yα-specific sequences are replaced by those of the opposite mating type (Figure 1). This process depends on the presence of two other mating type loci, the silent 'cassettes', *HMR*a and *HML*α. The structures of the *MAT* and *HML* loci are shown in Figure 1. The different regions have been defined by comparison of the nucleotide sequences of *MAT* and the cassettes (Hicks *et al.*, 1979; Nasmyth and Tatchell, 1980; Strathern *et al.*, 1980; Astell *et al.*, 1981). All three loci share the X (704 bp) and Z1 (239 bp) blocks, and *MAT* and *HML* also share the W (723 bp) and Z2 (89 bp) blocks. In most strains *HML* has Yα (747 bp) and *HMR* has Ya (642 bp), while *MAT* has either one. Repression of transcription of *HML* and *HMR* involves interactions between at least six *trans*-acting gene products and two *cis*-acting sites surrounding each of the two loci (reviewed by Strathern, 1988; Klar, 1989).

MAT conversion is initiated by a double-strand break (DSB) in the *MAT* locus, just to the right of the Y−Z1 junction, made by the HO endonuclease (Strathern *et al.*, 1982; Kostriken *et al.*, 1983; Kostriken and Heffron, 1984). The transcriptional repression of the cassettes also acts to protect them from HO cleavage and thus defines them as the donors, rather than recipients, of information in the *MAT* switching event (Klar *et al.*, 1981; Nasmyth, 1982). The HO-induced DSB is then repaired by copying information from an intact donor locus. This gene conversion event replaces the *MAT*−Y region as well as a variable amount of the W, X and Z regions (McGill *et al.*, 1989). In at least some of the switching events, the transfer of strands from the *HMR* or *HML* donor to *MAT* involves the formation of regions of heteroduplex DNA, as indicated by the post-switching segregation of restriction site markers in both the X and Z regions (McGill *et al.*, 1989). Selection of the cassette to be used as donor in the switch is directed by the mating phenotype of the cell and not specifically by the DNA sequences present at the *MAT* and cassette loci (Hicks and Herskowitz, 1976; Haber *et al.*, 1980; Rine *et al.*, 1981; Klar *et al.*, 1982; Jensen and Herskowitz, 1984; Tanaka *et al.*, 1984).

Current models for the mechanism of *MAT* switching are essentially special cases of the DSB repair model of recombination (Szostak *et al.*, 1983). There are two types of general models used to describe the mechanism of HO-induced *MAT* conversion. Both of these involve invasion of the donor by one or both strands of HO-cleaved *MAT* DNA, which are then extended by DNA synthesis using the donor's Y region as a template. The first model involves the HO endonuclease-induced DSB being enlarged into a gap by removal of the Y sequences, followed by the more-or-less simultaneous participation of both sides of the gapped DNA in strand invasion and replication of the intact donor strands (see Figure 2a) (Strathern *et al.*, 1982; Szostak *et al.*, 1983). Alternative models have been proposed that do not require degradation of the *MAT*−Y region as an early step in the switch. These invoke invasion of the cassette by the *MAT*−Z region and extension of this invading end by DNA synthesis using *HML* as the template (see Figure 2b). This DNA synthesis displaces a strand of the cassette, thus forming a 'D loop' which subsequently interacts with the *MAT*−WX region (Strathern *et al.*, 1982; Haber, 1983; Strathern, 1988). Once replication of the donor sequence progresses beyond the Y region into the *HML*-WX region, the displaced D loop strand can recombine with *MAT*−WX. A modified version of this model would include branch migration at the trailing end of a D loop to cause displacement of the newly synthesized strand rather than enlargement of the D loop (Szostak *et al.*, 1983; Strathern, 1988). The newly synthesized strand could recombine with *MAT*−WX sequences, leading to conservative replacement of the *MAT*−Y region by two newly synthesized DNA strands.

Using a galactose inducible HO gene (GAL-HO) carried on a plasmid (Jensen and Herskowitz, 1984) in cells

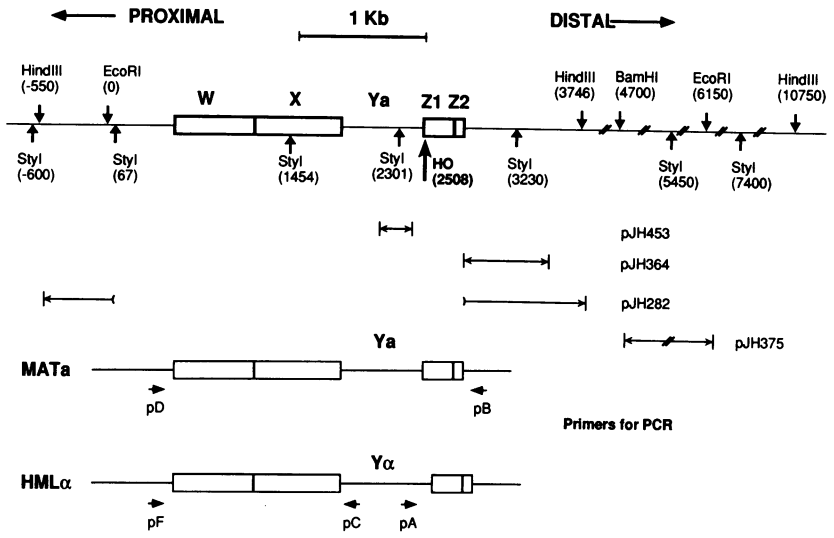

Fig. 1. Map of the *MAT* region of chromosome III. Relevant restriction sites, the site of HO cleavage, and the distances of these sites, in bp, from the *MAT* proximal *Eco*RI site are shown. The cloned fragments of *MAT*a DNA used for hybridization probes and the positions and orientations of oligonucleotides used for PCR are shown. Oligonucleotides pA and pC are homologous to Yα (*HMLα* and *MATα*), pB and pD are specific to the *MAT* locus and pF is speciic to the *HML* locus (see Materials and methods).

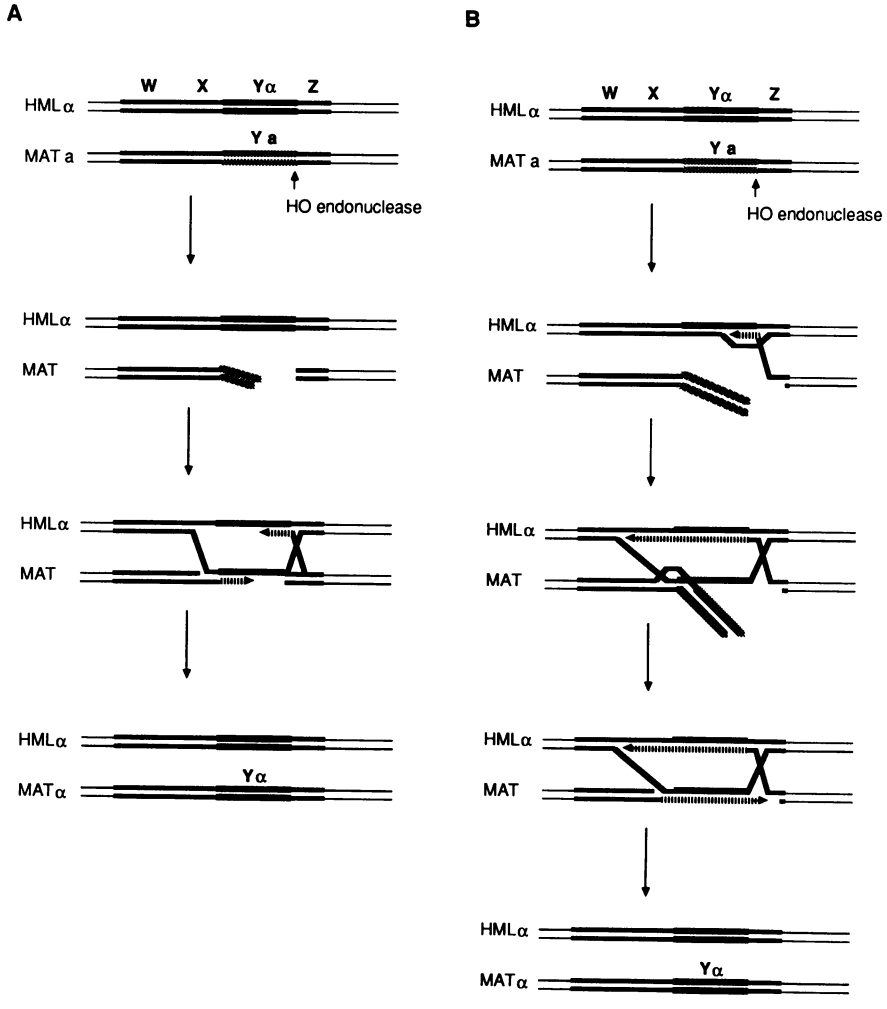

Fig. 2. Models of *MAT* switching. Double-strand gap repair (**a**) and one sided (**b**) models for *MAT* switching are shown. Following HO endonuclease cleavage of the *MAT* locus and degradation of the MAT−Y DNA, the gapped MAT locus is filled by simultaneous copying of the donor from both sides of the gap (a). Alternatively, in the absence of MAT−Y degradation, invasion of the donor by solely the MAT−Z end could proceed as shown. Evidence for (b) is presented here, allowing the exclusion of the simple double-strand gap repair model (see text). The W, X and Z regions are shown as heavy lines. The non-homologous Y regions are shown as thicker lines with Ya grey and Yα black. The railway tracks indicate new DNA synthesis.

otherwise unable to make HO endonuclease (*ho*), we have analysed the progress of the switch at the DNA level (Connolly *et al.*, 1988). This work has shown that 60 min elapse from the time of cutting of *MAT* to the appearance of the switched product. No evidence was found for degradation of the *MAT*−Y region prior to completion of the event. Similar results have also been found by D.Raveh and J.Strathern (personal communication). We now report the observation of two novel intermediates that provide the first molecular evidence of the way in which a programmed DSB initiates recombination. The first is a 5′−3′ exonucleolytic processing of one side of the HO-cleaved *MAT* DNA; the second is the subsequent invasion and primer extension of the resulting 3′ single-stranded DNA into the donor sequence. These results provide evidence that *MAT* switching does not proceed by the simultaneous participation of both sides of a DSB, as suggested by conventional DSB repair models, and point towards mechanisms in which the distal side of the HO cut is the more active agent in initiating recombination.

Results

Kinetics of MAT switching in RAD⁺ cells

Analysis of synchronously induced switching from *MAT*a to *MAT*α was carried out with R166 cells. In an effort to mimic as far as possible the 'normal' conditions of homothallic switching, the cells were held in the G1 cell-cycle phase with α factor during the period of HO induction. HO expression from the GAL-HO plasmid was induced by a 30 min exposure to galactose, following which the cells were washed into YEPD medium to repress HO expression and release them from the G1 block (see Materials and methods). The fraction of unbudded (G1 phase) cells immediately after washout into YEPD was 96%. As growth proceeded, this value dropped to a minimum of 22% in the 120 min time point sample and then increased to 78% in the last (240 min) sample. The 30 min induction was sufficient to induce *MAT*a to *MAT*α switches in 50% (19/38) of the cells.

DNA from each sample of these cells was digested with *Sty*I, which cleaves within *MAT*−Ya, but not *MAT*−Yα (Figure 1). The resulting DNA fragments were separated by electrophoresis on an alkaline agarose gel. Southern analysis of this gel, using the *MAT* distal probe (pJH364, see Figure 1) is shown in Figure 3a. The overall kinetics of the switch are as reported previously (Connolly *et al.*, 1988); the *MAT*α product is first seen 60 min after HO cleavage of *MAT*a. In addition, two transient bands of 2.9 and 4.9 kb appear sequentially, subsequent to *MAT* cutting and prior to the appearance of *MAT*α. Reprobing this filter with the *MAT*−Ya probe (see Figure 1) shows only the expected *HMR*a, *MAT*a and HO cleaved *MAT*a fragments (Figure 3b). Thus the transient, slower migrating bands are seen with *MAT* distal, but not *MAT* proximal probes. The autoradiogram shown in Figure 3a was scanned with a densitometer and the densities of the bands plotted in Figure 3c. This shows clearly the progress of the switch from *MAT*a, through HO cleavage of *MAT*a, to *MAT*α over the course of 60 min.

The transient intermediates contain long 3′-ended single-stranded ends

The transiently appearing bands are due to 5′−3′ degradation of the DNA distal to the cut. This degradation has the

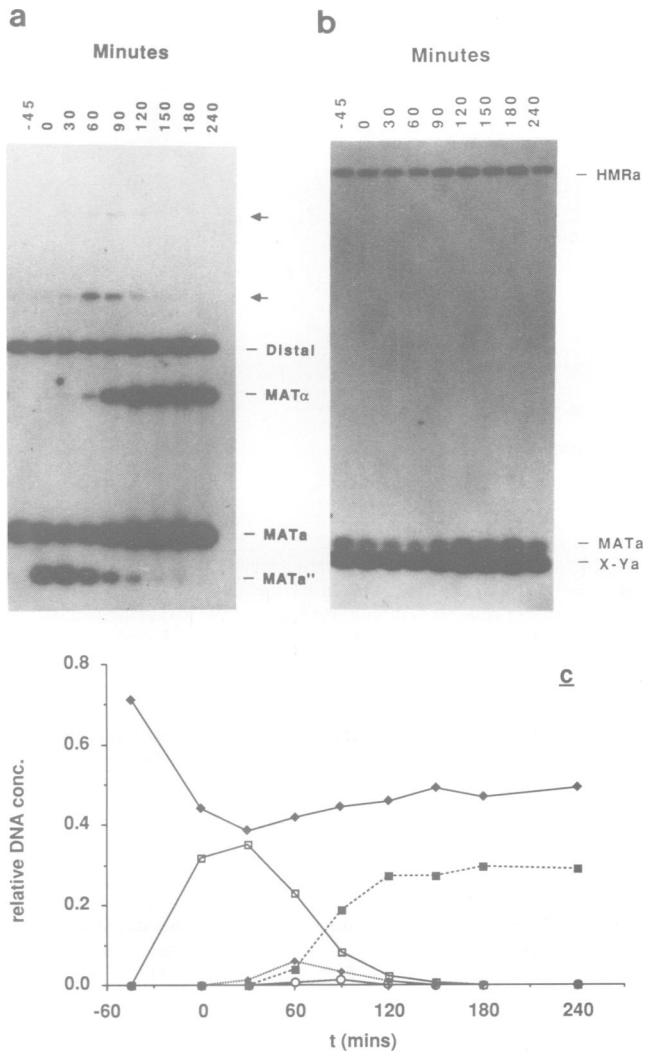

Fig. 3. Kinetics of *MAT* switching. (**a**) Autoradiogram of *Sty*I digested DNA samples from a time course with wild-type cells (R166). HO expression was induced for 30 min in an α factor blocked culture of wild-type cells, following which the cells were washed into YEPD (represses GAL-HO and releases the cells from the α factor block). The zero minute time point was taken immediately after resuspension of the cells in YEPD. DNA was prepared from samples taken at the indicated times and digested with *Sty*I. This DNA was electrophoresed through a NaOH−agarose gel, blotted and probed with the *MAT* distal probe (from pJH364, see Figure 1). The 930 bp *MAT*a fragment is cleaved by HO to give the 723 bp *MAT*a″ fragment. The product of the switch, *MAT*α (1880 bp), can first be seen 60 min after the initial *MAT* cleavage. Two transiently appearing higher molecular weight fragments of 2.9 and 4.9 kb are seen (indicated by arrows). The probe also hybridizes to a 2.2 kb fragment distal to *MAT*. (**b**) the blot used for (a) was washed and reprobed with the Ya probe (from pJH453, see Figure 1). This probe is homologous to both the *MAT*a and *HMR*a loci. *HMR*a, X−Ya (*MAT*a + *HMR*a) and *MAT*a fragments are seen. No transiently induced bands appear. Overexposure of this autoradiogram also failed to reveal any transient bands (not shown). (**c**) Densitometric scans ofthe autoradiogram shown in (a) were integrated, normalized to the sum of all *MAT* distal hybridizing bands and the resulting values plotted. The normalized 2.2 kb distal *Sty*I fragment remains approximately constant across the time course and was not plotted. Amounts of the 930 nt *MAT*a (solid line, ◆), 723 nt *MAT*″ fragment (solid line, □), 1880 nt *MAT*α product (dashed line, ■), and the 2.9 kb (dotted line, ◇) and 4.9 kb (solid line, ○) transient bands are shown).

effect of creating a 3′-ended single-stranded region refractory to restriction enzyme cleavage. The heterogeneous pool of partially degraded molecules therefore gives rise to a distinct

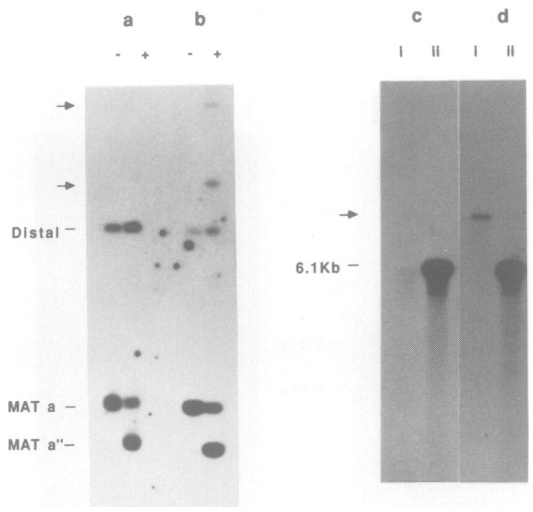

Fig. 4. Analysis of transiently appearing bands. (**a** and **b**) Alkaline gel analysis of *Sty*I digested DNA from HO-induced (60 min, +) and uninduced (−) cells probed with *MAT* distal (pJH364) stand-specific RNA probes: (a) complementary to the DNA strand 5′-ended at the HO cut; (b) complementary to the 3′-ended strand. These probes cover the same region as that used in Figure 3a and show the same bands (see Figure 3 legend). (**c** and **d**) *Hin*dIII and *Bam*HI digested DNA from HO-induced cells was separated on a neutral (TAE) gel. This gel was cut into slices and DNA was extracted from the slices by electro-elution. DNA from two of these slices, containing the ~8 kb transient band (i) and the 6.1 kb *Bam*HI−*Hin*dIII *MAT* distal fragment (ii; refer to Figure 1), was electrophoresed in duplicate on an alkaline agarose gel. This gel was blotted and the two duplicate strips were probed with *MAT* distal strand-specific RNA probes (pJH375; see Figure 1): (c) complementary to 5′-ended strand; (d) complementary to 3′-ended strand). The 3′-ended strand of the transient band migrates at the expected size of 8.2 kb (panel d i), and the other strand (panel c i) migrates as an indistinct smear from 6.1 kb down in size.

set of fragments for the 3′-ended strand on the denaturing gels, the sizes of which are determined by the more distal restriction endonuclease site that is still double stranded. This conclusion is based on the following observations: Firstly, examination of the restriction map of the *MAT* distal region (Figure 1) shows that these fragment sizes would be expected if there was loss of successive *Sty*I sites distal to the HO cleavage site. This also applies to the 8.2 kb band seen in *Hin*dIII digests (unpublished data). Furthermore, these fragments hybridize only to probes specific for the 3′-ended *MAT* distal strand at the HO cut. Two identical filters of *Sty*I digested DNA hybridized separately to pJH364 riboprobes specific for the 5′ and 3′-ended strands of *MAT* distal are shown in Figure 4a and b. The 2.9 and 4.9 kb bands hybridize only to probes specific for the 3′ *MAT* distal strand. Hybridization is not seen to probes specific for *MAT*−Ya (Figure 3b; see Figure 5b, in which similar bands are seen wtih the cassetteless strain), *MAT* proximal or *HML* distal (unpublished data).

To demonstrate that these fragments resulted from 5′−3′ rescission, a two-dimensional gel analysis was performed. DNA from cells induced with galactose was digested with *Hin*dIII plus *Bam*HI and separated on a neutral pH (TAE) agarose gel. This gel was cut horizontally into slices, and the DNA was extracted from each slice by electroelution. DNA from the two slices containing the 6.1 kb distal *Bam*HI−*Hin*dIII fragment and the ~8 kb transient band was then run on a denaturing gel. Southern analysis with strand

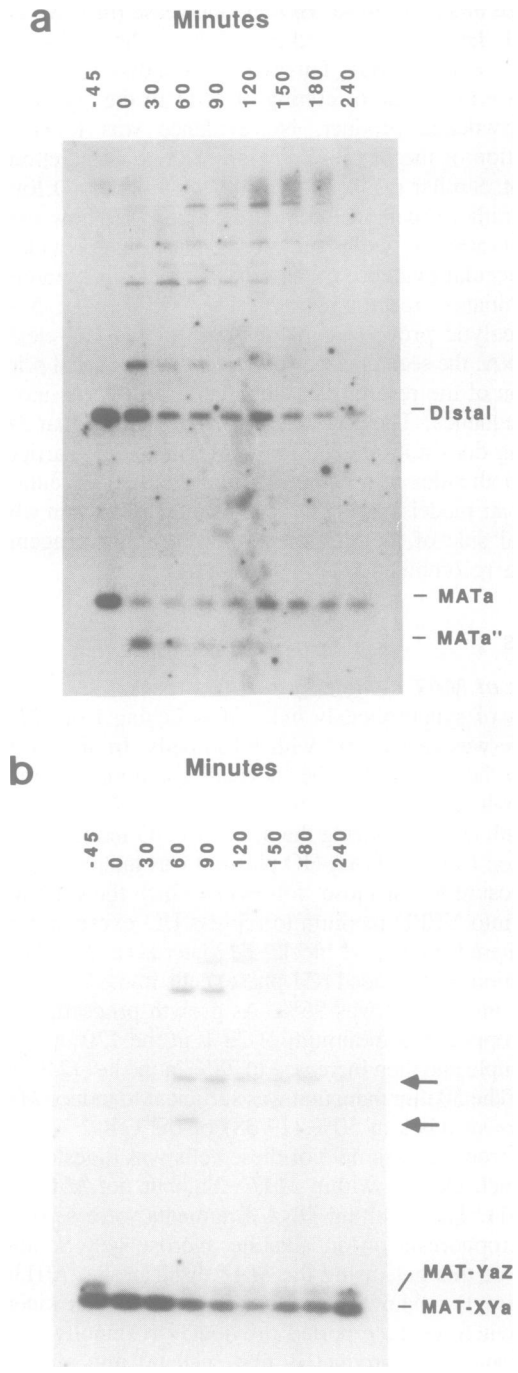

Fig. 5. (**a**) *rad52* time course. *Sty*I digested DNA from the *rad52* time course separated on an alkaline gel, blotted and hybridized to the *MAT* distal probe (pJH364, see Figure 3a). The 930 bp *MAT*a fragment is cleaved by HO to give the 723 bp *MAT*a″ fragment. No switching is seen in this strain and as expected, no *MAT*α DNA is produced. In contrast to the results with wild type cells (see Figure 3a), a series of progressively higher molecular weight bands is seen. The smallest two (and first to appear) of these corresponds to the 2.9 and 4.9 kb fragments seen in Figure 3a. The probe also hybridizes to a 2.2 kb fragment distal to *MAT*. (**b**) Cassetteless time course. Transient induction of HO in a derivative of the Rad$^+$ (WYL113-15b) strain in which both *HML* and *HMR* had been deleted. *Sty*I digested DNA from samples taken at the times shown was separated on an alkaline gel, blotted and hybridized to the *MAT*−Ya probe (pJH453, see Figure 1). In contrast to the results with wild-type cells (Figure 3b), a series of progressively larger high molecular weight bands are seen (indicated by arrows). X−Ya (*MAT*a) and *MAT*a−Z fragments are seen.

specific probes (Figure 4c and 4d) shows that the two DNA strands of the transient band are different in length: the 3′-ended (at the HO cut) strand is 8.2 kb, the expected size for a fragment extending from the HO cleavage site to the second distal *Hin*dIII site, and the 5′-ended strand shows as a smear with a maximum size of 6.1 kb.

Thus, following *MAT* cleavage by the HO endonuclease, a 3′-ended single-stranded tail is produced on the distal side of the HO cut by degradation of the 5′-ended strand. This single-stranded tail is homologous to the Z region of the donor, from which information is transferred by the switching event. Surprisingly, no such degradation is seen in the Ya sequences on the proximal side of the cut, which are not homologous to the Yα sequences of the donor. We believe that this asymmetry indicates that it is the distal side of the cleaved *MAT* locus which is initially active in the invasion of and transfer of information from the cassette.

The influence of the cassettes and RAD52 function on the degradation of the cleaved MAT strands

A possible explanation for the asymmetry seen in the degradation of the HO-cleaved *MAT*a is that it occurs subsequent to the invasion of the donor cassette locus (*HMLα*) by the 3′-ended distal strand of *MAT*a. Such invasion can only occur on the distal side of the cut, as the proximal side (Ya) is not homologous to *HML* (Yα). Invasion of the cassette by the 3′-ended distal *MAT* strand would leave the other (5′-ended) strand unpaired and thus accessible to single-strand specific endo- or exonucleases. An alternative explanation is that the degradation occurs prior to invasion of the cassette and serves to make the 3′-ended strand a more efficient invasion substrate, by virtue of its single strandedness.

In order to distinguish between these two possibilities, we constructed strain WYL113-15b, which lacks *HML* and *HMR* loci ('cassetteless'). As expected, this strain is unable to swtich mating type and dies upon attempting to do so (Klar *et al.*, 1984). Another function known to be involved in *MAT* switching is that of the *RAD52* gene, in the absence of which attempted switching is also lethal (Malone and Esposito, 1980; Weiffenbach and Haber, 1981). The *RAD52* gene, originally isolated as conferring X-ray sensitivity (Resnick, 1969; Game and Mortimer, 1974) is required for recombination and the repair of double strand DNA breaks in yeast (Ho, 1975; Resnick and Martin, 1976). An isogenic *rad52* strain was constructed by disruption of the *RAD52* gene (see Materials and methods). Although unable to switch mating type, it does have the cassettes and so serves to distinguish between effects due to lack of cassettes and those due to prolonged inability to switch. Furthermore, we hoped that examination of the Rad52$^-$ phenotype in this system would shed light on the specific function of the product of this gene. Time courses were carried out on these two strains in the same way as those done with the wild-type cells. A 30 min HO induction killed ~75% of the cells of both strains and induced no detectable mating type switches.

Figure 5a shows Southern analysis of *Sty*I digested DNA from the *rad52* time course probed with the *MAT* distal probe (pJH364). The contrast between the situation in these cells and that in the wild-type cells (see Figure 3a) is immediately apparent. Firstly, in agreement with the genetic data, no completed *MATα* product is seen; and secondly, higher molecular weight bands appear sequentially across the time

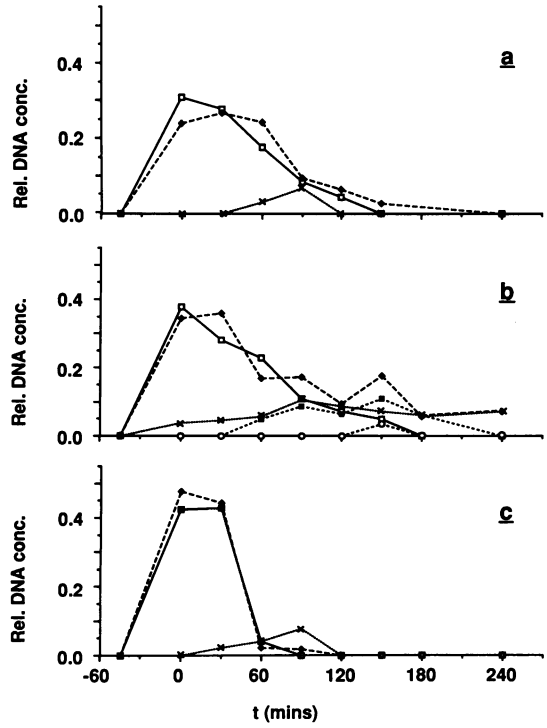

Fig. 6. Relative concentration of the *Hin*dIII *MAT* DNA fragments from *MAT*a to *MATα* switching time courses of the wild-type (**a**), *rad52* (**b**) and cassetteless (**c**) strains. DNA samples from the time courses of these three strains were digested with *Hin*dIII, separated on alkaline agarose gels, blotted, hybridized to the *MAT* surround probe (from pJH282, see Figure 1) and autoradiographed. Densitometric scans of the autoradiograms were integrated, normalized to the sum of all *MAT* distal hybridizing bands and the resulting values plotted. As there was substantial loss of *MAT*-hybridizing DNA in the cassetteless time course, normalization was done to the sum of the bands in the zero time point. Examination of the photograph of the ethidium bromide strained gel before Southern transfer and reprobing of this filter with a non-*MAT* (LEU2) probe showed that there was no substantial variation in the amount of DNA loaded across the time course (unpublished data). Relative concentrations of the 1.2 kb *MAT* distal (□), 2.8 kb *MAT*a proximal (◆) and 8.2 kb (x) transient fragments are shown. In the *rad52* time course two more transient bands of higher molecular weight were quantitated (■,○).

course. Probing this filter with strand specific probes (unpublished data) showed that these bands are, like the transient bands seen in the *RAD* time course, due to 5′−3′ degradation moving distally from the HO cleavage site. Thus the degradation distal to the HO cut site is not dependent upon *RAD52* function and is, in fact, more extensive in *rad52* cells. Hybridization of this filter to the Ya probe (pJH453) was carried out to determine whether or not the protection of the DNA strands proximal to the HO cut was dependent upon *RAD52* function. As with the wild-type strain (see Figure 3b), no proximal degradation was seen in the *rad52* cells (unpublished data).

Enhanced 5′−3′ degradation distal to the HO cut was also seen with the cassetteless strain (unpublished data). However, in contrast to the results in wild-type and *rad52* strains, the proximal side of the HO cut is not protected from exonucleolytic digestion. Higher molecular weight *Sty*I fragments homologous to a Ya probe are clearly evident in Figure 5b. As with the distal side, these bands arise by 5′−3′ degradation from the HO cut (unpublished data).

Southern analysis of *Hin*dIII digested DNA using the *MAT*

surround probe was carried out for the three strains. Densitometry was carried out and the results plotted in Figure 6. It can be seen that there is a pronounced difference between the cassetteless and the other two strains. The HO-cleaved *MAT* intermediates are rapidly lost in this strain. Thus the presence of the cassettes not only protects the proximal 5′ end and limits the distal 5′−3′ degradation, it also acts to protect the 3′-ended strands. The most simple explanation for this is that the distal 3′-ended strand is protected by its invasion of the cassette (for which it apparently does not need the *RAD52* gene product) and the proximal 3′-ended strand is protected by virtue of the protection of the proximal 5′-ended strand, with which it forms a duplex. Alternatively, a complex formed between *MAT* and the cassette, not dependent upon local DNA sequence homology, could act to protect the HO-cleaved ends. The protection of the proximal 5′-ended strand by interaction with a cassette, with which it shares homology at only the few terminal bases, implies that this is not by base pairing interactions. A possible candidate for this protection mechanism is the donor preference system (see Discussion).

The transfer of information to MAT is initiated from the distal side

The polymerase chain reaction (PCR), which acts to amplify a segment of DNA framed by two oligonucleotide primers, has two features that make it particularly suitable for the analysis of transient recombination intermediates: exquisite sensitivity allowing the practical detection of DNA species present at very low concentration, and the ability to amplify a defined DNA fragment of the desired length from within an heterogeneous population. If the invading strand(s) of *MAT* were extended by DNA synthesis using the cassette as template, our inability to visualize such structures by Southern analysis may have been due to the varied extent of synthesis in different cells. We hoped PCR analysis would enable us to amplify an homogeneous subfragment from this heterogeneous pool. Four oligonucleotide primers (20mers) were synthesized (see Materials and methods). Used as pairs these define two fragments of *MATα*: a distal fragment of 520 nucleotides (primers pA and pB) and a proximal fragment of 1497 bases (primers pC and pD; see Figure 1). Using PCR, we have analysed the temporal order of appearance of these two novel junctions at *MAT*.

In order to use the PCR quantitatively it was first necessary to determine the relationship between the amounts of starting material and the product of the amplification. To this end DNA samples from the beginning and end points of the time course were mixed in various proportions. These were amplified, separated on an agarose gel, the gel was stained and photographed, and the amounts of DNA were quantitated by densitometry (see Materials and methods). The results of three independent amplifications with both primer pairs show a linear relationship between starting and amplified DNA concentrations for both amplified fragments (Figure 7a). Thus it is possible to use PCR quantitatively to measure concentrations of these fragments in samples of genomic DNA.

We carried out three independent amplifications of time course DNA from R166 cells using each of the two primer pairs. The resulting material was run on agarose gels. Negatives of the gel photographs were scanned with the

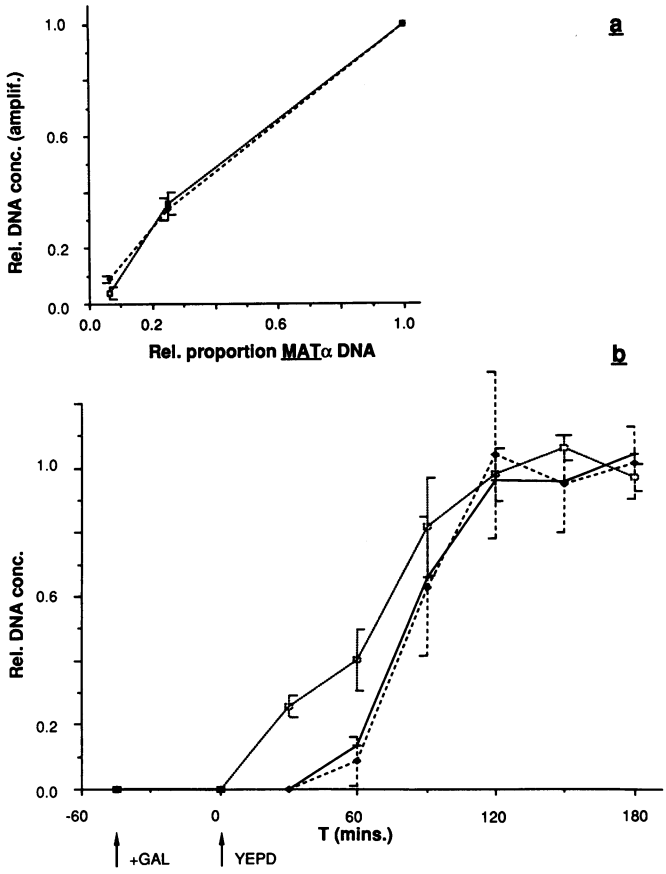

Fig. 7. (**a**) A linear relationship between the proportion of *MATα* DNA versus amount of PCR amplified fragment. DNA from the −45 and 180 min points of the wild-type switching time course were mixed in the proportions shown to give an increasing amount of *MATα* DNA in a constant total DNA concentration. Three independent amplifications of these mixtures were carried out with each of the two primer pairs: pA + pB (Yα−*MAT* distal) and pC + pD (*MAT* proximal−Yα). The amplified material was separated on agarose gels and stained with ethidium bromide, following which the UV fluorescence was photographed. Negatives were scanned with a densitometer and the resulting values were normalized to the 180 min time point sample (100%). Means and standard deviations were calculated from the three amplifications and these values plotted. Error bars are ± SD of the mean. (**b**) Quantitation of PCR amplified fragments of wild-type time course DNA. Means of three independent amplifications using the two primer pairs are plotted. Error bars are ±SD from the mean. Yα−*MAT* distal fragment (□); *MAT* proximal−Yα fragment (♦, dashed line). The solid line represents *MATα* DNA and is taken from the data shown in Figure 3c. As switching is completed by the 120 min time point, the average of values from the three last time points of each set of data was used to normalize the values for comparison. It can be seen that the distal junction of the switched product is formed earlier than the proximal junction, which appears coincidently with the completed *MATα* product (see text). The times at which galactose was added and the cells were washed into YEPD are indicated with arrows.

densitometer, mean and standard deviation values were calculated and the results were plotted in Figure 7b. The appearance of the completed *MATα* product quantitated from Southern analysis (Figure 3c) was also plotted. This graph shows a marked difference in the time of appearance of the two junctions: Yα−*MAT* distal appears ~30 min before both Yα−*MAT* proximal and the completed *MATα* product. As with the single-stranded intermediate described above, it is the distal side of the cut which is active before the proximal. These data indicate the presence of an intermediate

form in the switching process involving the joining of *MAT* distal DNA to Yα DNA in the absence of such joining on the proximal side.

This distal junction could have arisen in two ways: either DNA synthesis primed by the invading *MAT* strand or breakage of the displaced *HML* strand and ligation of this to the invading *MAT* strand(s). In the latter case, a contiguous DNA strand extending from *MAT* distal through *HML*−XW and into the *HML* distal region should be formed. Also, were DNA synthesis primed by the invading *MAT* strand to pass through *HML* and into the surrounding DNA, the former mechanism would also predict such a structure. We were unable to detect this structure by PCR using the *MAT* distal (pB) and *HML* distal (pF) primers. Control amplifications (not shown) of the *MAT* proximal (pD)−*MAT* distal (pB) fragment (2601 bp), showed that this was not due to an inability to synthesize a fragment of this length (2725 bp). Although lesser amounts may be present, it certainly is not produced stoichiometrically with the Yα-*MAT* distal fragment, as would be expected if they were the same structure. Thus we conclude that the *MAT* distal−Yα junction is formed by DNA synthesis, and not breakage-rejoining of the *MAT* and *HML* strands.

DNA from the *rad52* time course (see Figure 5a) was also examined by PCR as for the wild-type strain. Neither *MAT* distal−Yα nor *MAT* proximal−Yα junctions were detected using the *rad52* DNA samples. Amplified product was seen with a control pair of primers, which define a 682 bp fragment ~1 kb distal to *MAT* (unpublished data). We conclude that the *RAD52* gene product is required for the initial steps of strand invasion and/or DNA synthesis primed by this invading strand(s). This result is relevant to both the mechanism of protection of the 3′-ended distal strand and the function of the *RAD52* gene product (see Discussion).

Discussion

The recombination intermediates described here clarify our picture of the progress of the *MAT* conversion event. We describe two apparent intermediates in this process that follow the creation of a DSB by the HO endonuclease. The first is a 3′-ended single-stranded DNA extension on the distal, but not the proximal, side of the HO cut. The second is the formation of a covalent joint btween this end and the new (switched) Yα region prior to such joining on the other side of the cut.

The creation of the 3′-ended single-stranded region presumably occurs by the action of a 5′−3′ double-stranded DNA exonuclease. Aternatively, this strand may be unwound by a helicase activity and subsequently degraded by a single-strand specific nuclease. The effect of this is to produce a 3′-ended overhanging strand on the distal side of the HO cut, which bears homology to the donor cassette. We suggest that this degradation creates an efficient strand invasion substrate, with a 3′-OH end for priming DNA synthesis across the region of the cassette copied during the switch.

A considerable body of evidence suggests that a 3′-OH single stranded DNA end is an intermediate form in recombination in *Escherichia coli*. The recent view of prokaryotic recombination by Smith (1988) discusses this in detail, and only a brief summary will be given here. Activities implicated in recombination able to convert duplex DNA ends to 3′-ended, single stranded DNA overhangs include ExoV (*RecBCD*), ExoVIII (*RecE*) and λ exonuclease. Furthermore, the *sbcB* mutation, which suppresses the RecBC$^-$ hypo-rec phenotype, does this by suppressing the expression of ExoI, a 3′−5′ exonuclease.

There is some evidence that 3′-ended, overhanging strands also function as recombination intermediates in *Saccharomyces*. Two laboratories have recently reported purification of strand exchange activities from yeast cells (Kolodner *et al.*, 1987; Sugino *et al.*, 1988). One of these has been shown to have, as does the RecA protein of *E.coli*, a 3′−5′ strand exchange polarity with respect to the invading strand in assays of the transfer of a strand from duplex DNA (Kolodner *et al.*, 1987). The 3′-ended overhanging strand described here as a possible intermediate in *MAT* switching could be a substrate for this, or a similar, strand exchange activity. In addition, a site of initiation of meiotic recombination in yeast has recently been identified (Nicolas *et al.*, 1989) and broken DNA ends with 3′-ended single stranded overhangs several hundred bases long were seen at or near this site (Sun *et al.*, 1989; H.Sun and J.Szostak, personal communication). Similar 3′ overhangs at the site of a double strand break have been seen in linear plasmid DNA injected into *Xenopus laevis* oocytes (Maryon and Carroll, 1989).

In our experiments, we only detect that fraction of the exonucleolytic processing events that extend at least 700 bp, proceeding outside of the *MAT*−Z region. During normal switching these extensive degradation products accumulate to only 15% of the final product. Creation of such an extensive single-stranded tail in this fashion certainly does not interfere with switching, as this is what happens when cells blocked from DNA repair by hydroxyurea, are released and switch efficiently (Connolly *et al.*, 1988). Nevertheless, we do not wish to suggest that induction of strand invasion by the 3′ end requires such extensive degradation of the opposite strand of DNA. The presence of a long 3′ single-stranded region requiring recopying using either *HML* or *MAT* strands as template is consistent with the recent report of frequent gene conversions or post-switching segregation of a Z region marker close to the HO cut site (McGill *et al.*, 1989).

Protection of the distal side of the HO cut is donor dependent

The 5′−3′ degradation seen distal to the HO cut was not seen on the proximal side (*MAT*−Ya). This protection of the *MAT*−Ya strands depends on the presence of the cassette and is independent of the *RAD52* function. The absence of proximal degradation in the *rad52* strain is particularly striking given the extent of degradation seen distal to the HO cut in these cells. The protected Ya strands are not homologous to the *HML*−Yα region, so the protection cannot be due to base pairing interactions. The proximal 3′-ended strand is also stable in a cassette dependent, *RAD52* independent manner. It is possible that the 3′-ended strand is stabilized by virtue of being duplex, in that it is lost subsequent to degradation of the proximal 5′-ended strand in the cassetteless strain. Alternatively, a *MAT*−cassette complex, not involving base pairing interactions around the HO cut, may be acting *in vivo* to exclude 3′−5′ exonucleases. If the protection is mediated by protein(s) binding to the protected end, such binding is not resistant to our DNA extraction procedures, as the HO-cleaved *MAT* DNA is degraded *in vitro* by both 5′−3′ (λexo and T7 gene

6 exo) and 3′−5′ exonucleases (T4 DNA Polymerase) (unpublished data).

The major argument for the functional significance of this degradation is its asymmetry and the dependence of this asymmetry upon the presence of the donor. Only the distal 5′-ended strand is visibly degraded, and the extent of degradation seen is influenced by the cell's ability to complete the switching event. If, as we suggest, the function of this is to create a 3′ overhang to act as the invading strand in the *MAT* conversion event, degradation of the proximal 5′-ended strand would have the undesirable effect of creating an efficient substrate for the invasion of the wrong cassette, as the unswitched *MAT*−Ya region is homologous to the Ya region of the *HMR*a cassette not used as donor in the switch. Thus there is a cassette-dependent mechanism in these cells which protects one side of the HO cut *MAT* but not the other. Another relevant observation comes from studies of cells induced to switch in the presence of the DNA synthesis inhibitor, hydroxyurea (HU), which fail to switch until released from the drug (Connolly *et al.*, 1988). Examination of *Hin*dIII digested DNA from these cells has shown that the HU block causes an accumulation of the degraded strand form (C.White and J.Haber, unpublished). Accumulation of this structure does not interfere with normal progress of the switching event, since upon release these cells are able to complete switching with apparently normal kinetics (Connolly *et al.*, 1988).

One possible way in which cassette-mediated protection of the Ya strands might occur would be through sites and *trans*-acting factors that specify donor preference, whereby *MAT*a preferentially uses *HMLα* as donor and *MATα* uses *HMR*a. Like the cassette-dependent protection of the *MAT*−Y DNA strands, the selection of the correct cassette locus to act as donor in the switch is apparently not due to homologous DNA interactions between *MAT* and the cassette but depends on sites flanking the donor (J.E.Haber, W.X.An, X.W.Wu and R.M.Dempsey, manuscript in preparation). It is possible that the pairing of *MAT* and its donor form a complex that prevents access of exonucleases to the *MAT*−Y region until late in the gene conversion process.

Role of the RAD52 gene in MAT switching

The 3′-ended overhanging strand distal to the HO cut is stable in a cassette-dependent, but *RAD52*-independent manner. Furthermore, the *RAD52* function is required at a stage prior to the priming of synthesis by the invading strand(s), as no *MAT* distal−Yα PCR product was obtained from the *rad52* time course DNA. Thus we suggest two possible functions for *RAD52*. If the protection of the distal 3′-ended strand is due to its base pairing with *HML* in an invasion structure, *RAD52* is required for the initiation of synthesis at this end. Alternatively, the protection of this end may be due to its interaction with the cassette in some form of pre-synaptic complex. In this case, *RAD52* function would be required to convert this to a fully synapsed structure (by catalyzing strand invasion?). Observation of cassette-dependent, homology-independent protection of the *MAT*−Y strands proximal to the HO cut, leads us to believe that the latter explanation or *RAD52* function is more likely (see below).

The *RAD52* gene is required for most mitotic recombination events (Malone and Esposito, 1980; Jackson and Fink, 1981). Haber and Hearn (1985) reported that mitotic recombination events in *rad52* diploid cells were reduced 50-fold. Those that do occur were frequently associated with chromosome loss, which could be explained by the failure to complete recombination events correctly. In these experiments, as well as those reported by Hoekstra *et al.* (1986), the types of recombination events that occurred were markedly different from those seen in wild-type cells. These differences were interpreted as arising from the formation of longer regions of heteroduplex DNA (Haber and Hearn, 1985; Hoekstra *et al.*, 1986). Our observation that *rad52* cells create more extensive single-stranded regions adjacent to DSBs is consistent with these genetic conclusions. It should be noted that a yeast nuclease, expression of which seems to be positively regulated by the *RAD52* gene (Chow and Resnick, 1988), is apparently not the activity causing the 5′−3′ degradation during *MAT* switching as this degradation is enhanced in *rad52* mutant cells.

Strand invasion and primer extension occur first on one side of the HO cut

Following invasion, the junction between the distal side of *MAT* and the Yα sequence is formed prior to that on the proximal side. This junction might have been formed either by DNA synthesis primed by the invading *MAT* distal strand(s) using *HML*−Yα as template, or by breakage and rejoining of the displaced *HML* strand and the invading *MAT* strand. In the latter case, a contiguous *MAT* distal−*HML* distal strand would be formed and remain until resolved by interaction between the *MAT*− and *HML*−W or −X regions. We were unable to detect this DNA species and conclude that the *MAT* distal−Yα junction is formed by DNA synthesis. In agreement with this, cells blocked with the DNA synthesis inhibitor hydroxyurea (Connolly *et al.*, 1988; C.White, unpublished) accumulate the distal single stranded end, indicating that DNA synthesis is required for the formation of the Yα−*MAT* distal covalent strand(s). The *MAT* proximal−Yα junction appears ~30 min later, coincident with the completed *MATα* product of the switch. It is tempting to speculate that the one strand of the distal junction is formed early by extension of the invading 3′-ended strand, and that the other strand is formed later by gap filling of the structure shown in Figure 2. Further experiments able to distinguish whether the 3′ end is that which is first joined to Yα sequences are currently underway.

Relation of the observed intermediates to models of MAT switching

This sequence of events contrasts to that proposed by the simple double-strand gap repair model for switching (Figure 2a) (Strathern *et al.*, 1982; Szostak *et al.*, 1983), in that only the distal side of the cut appears to be active in the invasion of the cassette. Our data are consistent with models invoking displacement of a strand of the donor by DNA synthesis primed by an invading end of *MAT* DNA (Strathern *et al.*, 1982; Haber, 1983;Szostak *et al.*, 1983; Strathern, 1988). These data are also consistent with the interpretations offered to explain the recent observations of McGill *et al.* (1989) that co-conversion of a restriction site marker 26 bp in the Z region is less frequent than co-conversion of markers 54 and 229 bp from the Y−X border. This difference in the likelihood of a site being co-converted may reflect differences in the way recombinational interactions occur in the Z region (where it appears switching is initiated) and in the X region.

We are unable to determine whether or not the newly synthesized strand copied from *HML* is displaced by branch migration from the trailing end of a small D loop or remains paired with a donor template strand until branched structures are resolved at the end of the switching process. Recent data by McGill *et al.* (1989) appear less compatible with the displacement of the newly synthesized strand, based on the observation that in cases where there is evidence of heteroduplex DNA on both sides of the Y region, the marker originally found at *MAT* is on opposite strands in Z than in X. We are unsure if these data are strong enough to rule out this version of a mechanism, as there were only 3/60 informative events, and at least 15% of the events involving conversions and post-switching segregations of the X region marker appear to have had more than one HO-induced switch.

GAL-HO induced MAT switching is a slow event

To date, we have been able to identify at least three kinetically slow steps in the process of *MAT* switching: the appearance of HO cleaved fragments, the 5′−3′ rescision of the distal region and the formation of a covalent joint between Yα sequences from the donor to the *MAT*−Z region. We have not as yet directly identified other possible intermediate structures such as Holliday junctions, but note that there is still 30 min from the time in which the first joining of *MAT* to donor sequences occurs and the completion of the event. As we have discussed earlier (Connolly *et al.*, 1988), the time taken for completion of this event (60 min) may seem surprising. Whether *GAL-HO* induced switching differs kinetically from the natural *HO*-induced events is not known, as it has not been possible to follow *MAT* conversion in synchronized cells with normal cassettes and the normal *HO* gene. By all genetic criteria the *GAL-HO* induced events appear to be normal: there is no lethality associated with galactose induction and G1 cells give rise to a pair of cells, both of which have switched to the same mating type (see discussion by Connolly *et al.*, 1988). Galactose-induced switching also obeys the same donor preference rules, in that *MAT*a cells switch preferentially to *MAT*α rather than to *MAT*a (Connolly *et al.*, 1988; also Dempsey and Haber, unpublished results). The fact that there are so many apparently slow steps (this work) makes it unlikely that galactose induction of *HO* has dissociated its expression from one other, rate-limiting recombination enzyme. Similar slow kinetics have been observed for HO-induced double strand break repair of plasmid-borne LacZ sequences (Rudin *et al.*, 1989) as well as recombinational repair of an HO-induced chromosomal break (Rudin and Haber, 1988). Persistent (that is, readily detectable) double-strand breaks at the sites of meiotic 'hot spots' have also been observed in meiotic cells undergoing recombination (Sun *et al.*, 1989).

It has been previously assumed that *MAT* switching should occur rapidly, based on the observation of a low (1−2%) steady state level of detectable double strand break in homothallic cells that are capable of switching continuously (Strathern *et al.*, 1982). However, because cells switching from *MAT*a to *MAT*a cannot be distinguished from cells that did not switch at all, it is not in fact known what proportion of *HO MAT*a *HML*a *HMR*a cells actually do switch. Moreover, recent evidence from F.Heffron (personal communication) suggests that HO gene expression may be autoregulated, so that possibly only a small fraction of cells in such a supposedly continuously switching poulation are actually undergoing switching. Nevertheless, because yeast cells exhibit high levels of all forms of homologous recombination, we cannot rule out the possibility that the *GAL-HO* induced events occur by a highly efficient, more general pathway of double-strand break repair than what occurs following expression of the normally regulated *HO* gene. Clearly, *MAT* switching does have certain special features, most notably the regulated pairing of *MAT* with one of two possible donors and a constraint on crossing-over accompanying gene conversion; however, it appears that *MAT* switching requires essentially all of the same gene functions as does other mitotic recombination events, including *RAD52* and other radiation-repair genes (reviewed by Haber, 1983; also C.I.White and J.E.Haber, unpublished observations).

The slowness of *MAT* switching apparently does not pose a problem for cells with a normal doubling time of 2−3 h. Recently, Weinert and Hartwell (1988) have shown that the *RAD9* gene is part of a system that detects DNA damage and arrests cells prior to mitosis to allow such repair to occur. After DNA damage by irradiation, there is a marked arrest of cells while such damage (as little as one or a few lesions per cell) is repaired. That such DNA repair also appears to be a slow process is consistent with what we observe for the more specific case of *MAT* switching. Even after *MAT* switching is clearly in mid-process, i.e. when *MAT* distal becomes joined to Yα, the remaining steps in the process are slow. We suspect that during this time one might be able to detect the formation of branched DNA structures such as Holliday junctions.

The data presented here argue that *MAT* switching is initially driven by the activation of one side of the HO-induced cut at *MAT*. The constraints on the exonucleolytic processing of the *MAT*−Y region involve an interaction with the silent copy donor. This protection may be specific to the *MAT* system or may be a more general consequence of pairing of homologous regions. Studies of HO-induced recombination between *LacZ* sequences in yeast are also consistent with the majority of such events being 'one-ended' rather than 'two-ended' (Rudin *et al.*, 1989). It is hoped that further analysis of these events will determine the generality of this mechanism.

Materials and methods

Media

Cells were grown in YEP (1% w/v yeast extract, 2% w/v Bacto-peptone) supplemented with dextrose (2% w/v, YEPD) or lactic acid (3.15% w/v pH 5.5, YEPL). To induce the GAL-HO gene, galactose (2% w/v) was added to YEPL media. Synthetic complete medium lacking uracil (SC-uracil) was made according to Sherman *et al.* (1983). Bacto-Agar was added (2% w/v) for solid media.

Strains

R166 was obtained by transformation of BWG1-7a (*ho HML*α *MAT*a *HMR*a *leu2*-3, 112 *ura3*-52 *his4*-519 *ade1*-100 GAL) with the GAL-HO plasmid (pJH132). BWG1-7a was a gift from L.Guarente. The *rad52* strain, TCW7-3, was constructed by transformation of BWG1-7a with the *rad52*::*LEU2 Bam*HI fragment of pSM20 (Schild *et al.*, 1983). pSM20 was kindly provided by D.Schild. Leu$^+$ transformants were single colony purified and checked for γ-ray sensitivity. One of the γ-ray sensitive clones was transformed with pJH132 to give TCW7-3 (*ho, HML*α, *MAT*a, *HMR*a, *leu2*-3,112, *ura3*-52, *his4*-519, *ade1*-100, *rad52*::*LEU2*, GAL, pGAL-HO). A strain with both cassettes deleted was constructed (WYL113-15b). First

a plasmid with an *hml* deletion was built by deleting the 5.3 kb *Xho*I fragment spanning the *HML* locus from a plasmid containing the 6.5 kb *Bam*HI *HMLα* fragment. The 2.1 kb *LEU2 Sal*I−*Xho*I fragment was inserted into this site to make pJH455 (*hmlΔ* :: *LEU2*). Feldman *et al.* (1984) have published a detailed restriction map of this region. R166α (GAL-HO induced switch of R166 from *MAT*a to *MAT*α) was transformed with the *Bam*HI fragment of pJH455, Leu$^+$ transformants were selected and checked to be *hmlΔ* :: *LEU2* by Southern analysis. The resulting *MATαhmlΔ* strain was mated with R126 (Connolly *et al.*, 1988), which carries the *hmr* deletion allele, *hmr*-3Δ (Klar *et al.*, 1982). Yeast cells were transformed using lithium acetate (Ito *et al.*, 1983). This diploid was sporulated, and Leu$^+$ Ura$^+$ segregants were tested for galactose sensitivity, as HO expression is lethal in cassetteless strains (Klar *et al.*, 1984). Candidates were checked by Southern analysis and WYL113-15b (*hmlΔ* :: *LEU2 MAT*a *hmr*-3Δ *leu2 trp1 ura3-52 thr4 his4 ade1* GAL *URA3-GAL-HO*) was chosen for subsequent use.

Plasmids

All strains carry the GAL-HO plasmid (URA3 ARS1 CEN4 GAL-HO) (Jensen and Herskowitz, 1984). pJH282 has 1.6 kb of *MAT*-specific sequences, derived from the *Hin*dIII *MAT* fragment by deleting the W,X,Y and Z sequences; the resulting 1.6 kb *Hin*dIII fragment is inserted into the *Hin*dIII site of pGEM3. Ya specific pJH453 has the 383 bp *Ssp*I−*Bgl*II *MAT*−Ya fragment inserted into *Bam*HI/*Hin*CII digested pGEM3. pJH364 has a *MAT* distal fragment including 52 bp of *MAT*−Z2, extending 647 bp distally to a *Hae*III site. pJH452 has the 1450 bp *MAT* distal *Bam*HI−*Eco*R1 fragment inserted into *Bam*HI/*Eco*R1 cut pGEM3. These insert fragments are shown in Figure 1.

Induction of MAT switching

YEPL medium was inoculated from a late log-phase SC-uracil culture and shaken at 30°C overnight to a cell density of $2-4 \times 10^6$ cells/ml. Alpha factor (Sigma Chemical Co., 1 mg/ml in Ethanol) was added to 1 μg/ml, and cellular morphology was monitored until the proportion of budded cells in the population dropped below 5%, indicating that the majority of the cells were in the G1 phase. An aliquot of cells was removed for the zero time point. Galactose (1/10 vol. of 20% w/v) was added to the remainder and incubation continued. After 30 min the cells were harvested onto a sterile nitrocellulose filter (0.4 μm pore, Millipore Corp.), washed with pre-warmed YEPD and resuspended in YEPD medium. Incubation was then continued, and samples were withdrawn at the given times. As the HO enzyme is rapidly turned over (Connolly *et al.*, 1988), this is essentially a pulse−chase time course.

Appropriate dilutions of the cells were made into sterile water, and these were plated on YEPD and SC-uracil to measure both total and Ura$^+$ cell numbers. Individual colonies were picked and their mating type determined by crossing to tester strains with the relevant markers (Sherman *et al.*, 1983).

DNA extraction

Cells from 40 ml ($\sim 5 \times 10^7 - 1 \times 10^8$ cells) of each sample were harvested onto a nitrocellulose filter and washed with TE (10 mM Tris−HCl, 1 mM EDTA, pH 7.4). Resuspension of the cells was carried out by vortexing the filter in 0.5 ml 'Ex' buffer (100 mM Tris−HCl, pH 8.0, 50 mM EDTA, 2% SDS) in a 1.5 ml micro-centrifuge tube. Glass beads (0.45−0.5 mm diameter, acid washed and baked) were added to the level of the meniscus, 0.5 ml TE-saturated phenol/chloroform/isoamyl alcohol (25:24:1) was added, and the tube was vortex-mixed for 2 × 20 s and cooled on ice. The aqueous phase was extracted twice more, made 0.3 M in sodium acetate (NaOAc), and the DNA was precipitated with 2 vol. of ethanol. Care was taken to avoid carrying over any material from the interface in the extractions. The precipitate was pelleted, dissolved in TE, treated with pancreatic RNaseA (100 μg/ml; 30 min, 37°C), phenol/chloroform extracted and NaOAc−ethanol precipitated. The purified DNA was dissolved in TE and stored at −20°C.

Electrophoresis

Neutral agarose gels were prepared and run in 40 mM Tris−acetate, 2 mM EDTA (TAE; Maniatis *et al.*, 1983). Alkaline agarose gels were as described by McDonnel *et al.* (1977). All gels included molecular weight marker lanes (one or both of Lambda−*Hin*dIII or φX174−*Hae*III; from New England Biolabs). In order to eliminate the possibility of cross hybridization with labelled marker DNA, a ruler laid on the gel when the photograph of the ethidium bromide fluorescence was taken was used to determine the positions of the marker bands relative to the origin.

Purification of DNA from gels

Gel slices in TAE buffer in closed bags of dialysis tubing (Spectra/por #3, Spectrum Medical Industries, CA, USA) were submerged in this buffer in a horizontal electrophoresis chamber. Voltage (7 V/cm) was applied for 60 min, reversed for 30 s and the DNA was recovered by precipitation with NaOAc−ethanol (McDonnel *et al.*, 1977, with modifications).

Southern analysis

Restriction endonuclease digested DNA was electrophoresed in agarose gels and transferred overnight to nylon membrane ('Zetaprobe', Biorad) in 0.4 M NaOH (Reed and Mann, 1985). Hybridization and washing of filters was carried out by the method of Church and Gilbert (1984). Unless specifically stated, ^{32}P-labelled hybridization probes were prepared using the random primer method (Feinberg and Vogelstein, 1983, 1984) with either the Biorad or Boehringer Mannheim kit. DNA restriction fragments for random primer probe synthesis were isolated from agarose gels. Strand-specific ^{32}P-labelled RNA probes were prepared with the SP6 or T7 RNA polymerases (Melton *et al.*, 1984) using the 'Riboprobe' kit (Promega Biotec) according to the manufacturer's instructions. Filters were autoradiographed using standard procedures (Maniatis *et al.*, 1983). Densitometry of autoradiograms was carried out using a Biorad Model 620 Video Densitometer.

PCR

The PCR (Saiki *et al.*, 1985, 1988; Scharf *et al.*, 1986) was carried out using the 'GeneAmp DNA Amplification Kit' under the conditions specified by the manufacturer (Perkin Elmer Cetus, Norwalk, CT, USA). Master mixes of all components except DNA were made to avoid variation due to pipetting errors. Standard PCR was with ~5 ng of genomic DNA for 25 cycles (each: 1.5 min, 94°C; 2 min, 55°C; 3 min, 72°C), followed by 7 min at 72°C. The samples were allowed to cool to room temperature, the aqueous phase was extracted with phenol−chloroform, and DNA was precipitated with NaOAc−ethanol. Pellets were resuspended in TE and electrophoresed on neutral agarose gels. The gels were stained with ethidium bromide and photographed on a UV trans-illuminator. Quantitation of the DNA was by densitometry of the negative (see above).

Oligonucleotide primers (20mers) were synthesized using the 'cyclone' DNA synthesizer (MilliGen/Biosearch, Millipore Corp.) based on the known DNA sequence of the *MAT* and *HML* loci (Astell *et al.*, 1981; Feldman *et al.*, 1984; C.White, unpublished). The oligomers made are: pA (pGCAGCACGGAATATGGGACT); pB (pATGTGAACCGCATGGGCAGT); pC (pAGATGAGTTTAAATCCAGCA); pD (pTGTTGTCTCACTATCTTGCC); pF (pATCTAGCGCACATAGAATGA). The positions of these sequences in the *MAT* region are shown in Figure 1. Examination of the sequence of the *MAT Eco*RI−*Hin*dIII DNA showed that these sequences are unique within this DNA fragment.

Acknowledgements

Preliminary experiments were also performed with B.Connolly. We thank W.-D.Heyer, M.Lichten, B.Ray, N.Sugawara, J.Fishman, F.W.Stahl and the Eugene recombination club for helpful comments on the manuscript and W.-Y.Leung for constructing the cassetteless strain. This work was supported by NIH grant GM20056.

References

Astell,C.R., Ahlstrom-Jonasson,L., Smith,M., Tatchell,K., Nasmyth,K.A. and Hall,B.D. (1981) *Cell*, **27**, 15−23.
Chow,T.Y. and Resnick,M.A. (1988) *Mol. Gen. Genet.*, **211**, 41−48.
Church,G.M. and Gilbert,W. (1984) *Proc. Natl. Acad. Sci. USA*, **81**, 1991−1995.
Connolly,B., White,C.I. and Haber,J.E. (1988) *Mol. Cell. Biol.*, **8**, 2342−2349.
Feinberg,A.P. and Vogelstein,B. (1983) *Anal. Biochem.*, **132**, 6−13.
Feinberg,A.P. and Vogelstein,B. (1984) *Anal. Biochem.*, **137**, 266−267.
Feldman,J.B., Hicks,J.B. and Broach,J.R. (1984) *J. Mol. Biol.*, **178**, 815−834.
Game,J.C. and Mortimer,R.K. (1974) *Mutat. Res.*, **24**, 281−292.
Haber,J.E. (1983) In Adya,S.L., Bukhari,A.I. and Shapiro,J.A. (eds), *Mobile Genetic Elements*. Academic Press, New York, pp. 559−619.
Haber,J.E. and Hearn,M. (1985) *Genetics*, **111**, 7−22.
Haber,J.E., Savage,W.T., Raposa,S.M., Weiffenbach,B. and Rowe,L.B. (1980) *Proc. Natl. Acad. Sci. USA*, **77**, 2824−2828.
Hicks,J.B. and Herskowitz,J. (1988) *Genetics*, **83**, 245−258.
Hicks,J.B., Strathern,J.N. and Klar,A.J. (1979) *Nature*, **282**, 478−483.
Ho,K.S.Y. (1975) *Mutat. Res.*, **30**, 327−334.
Hoekstra,M.F., Naughton,T. and Malone,R.E. (1986) *Genet. Res.*, **48**, 9−17.

Ito,H., Fukuda,Y., Murata,K. and Kimura,A. (1983) *J. Bacteriol.*, **153**, 163–168.
Jackson,J.A. and Fink,G.R. (1981) *Nature*, **292**, 306–311.
Jensen,R.E. and Herskowitz,I. (1984) *Cold Spring Harbor Symp. Quant. Biol.*, **49**, 97–104.
Klar,A.J.S. (1989) In Berg,D.E. and Howe,M.M. (eds), *Mobile DNA*. American Society for Microbiology, Washington, D.C., p. 671–691.
Klar,A.J., Strathern,J.N. and Hicks,J.B. (1981) *Cell*, **25**, 517–524.
Klar,A.J., Hicks,J.B. and Strathern,J.N. (1982) *Cell*, **28**, 551–561.
Klar,A.J., Strathern,J.N. and Abraham,J.A. (1984) *Cold Spring Harbor Symp. Quant. Biol.*, **49**, 77–78.
Kolodner,R., Evans,D.H. and Morrison,P.T. (1987) *Proc. Natl. Acad. Sci. USA*, **84**, 5560–5564.
Kostriken,R. and Heffron,F. (1984) *Cold Spring Harbor Symp. Quant. Biol.*, **49**, 89–104.
Kostriken,R., Strathern,J.N., Klar,A.J., Hicks,J.B. and Heffron,F. (1983) *Cell*, **35**, 167–174.
Malone,R. and Esposito,R.E. (1980) *Proc. Natl. Acad. Sci. USA*, **77**, 503–507.
Maniatis,T., Fritsch,E.F. and Sambrook,J. (1983) *Molecular Cloning. A Laboratory Manual*. Cold Spring Harbor Laboratory Press, Cold Spring Harbor, NY.
Maryon,E. and Carrol,D. (1989) *Mol. Cell. Biol.*, in press.
McDonnel,M.W., Simon,M.N. and Studier,F.W. (1977) *J. Mol. Biol.*, **110**, 119–146.
McGill,C., Shafer,B. and Strathern,J.N. (1989) *Cell*, **57**, 459–467.
Melton,D.A., Krieg,P.A., Rebagliati,M.R., Maniatis,T., Zinn,K. and Green,M.R. (1984) *Nucleic Acids Res.*, **12**, 7035–7056.
Nasmyth,K.A. (1982) *Cell*, **30**, 567–578.
Nasmyth,K.A. and Tatchell,K. (1980) *Cell*, **19**, 753–764.
Nicolas,A., Treco,D., Schultes,N.P. and Szostak,J.W. (1989) *Nature*, **338**, 35–39.
Reed,K.C. and Mann,D.A. (1985) *Nucleic Acids Res.*, **13**, 7207–7221.
Resnick,M.A. (1969) *Genetics*, **62**, 519–531.
Resnick,M.A. and Martin,P. (1976) *Mol. Gen. Genet.*, **143**, 119–129.
Rine,J., Jensen,R., Hagen,D., Blair,L. and Herskowitz,I. (1981) *Cold Spring Harbor Symp. Quant. Biol.*, **45**, 951–960.
Rudin,N. and Haber,J.E. (1988) *Molec. Cell. Biol.*, **8**, 3918–3905.
Rudin,N., Sugarman,E. and Haber,J.E. (1989) *Genetics*, **122**, 519–534.
Saiki,R.K., Scharf,S.J., Faloona,F., Mullis,K.B., Horn,G.T., Erlich,H.A. and Arnheim,N. (1985) *Science*, **230**, 1350–1354.
Saiki,R.K., Gelfand,D.H., Stoffel,S., Scharf,S.J., Higuchi,R., Horn,G.T., Mullis,K.B. and Erlich,H.A. (1988) *Science*, **239**, 487–491.
Scharf,S.J., Horn,G.T. and Erlich,H.A. (1986) *Science*, **233**, 1076–1078.
Schild,D., Konforti,B., Perez,C., Gish,W. and Mortimer,R. (1983) *Curr. Genet.*, **7**, 85–92.
Sherman,F., Fink,G.R. and Hicks,J.B. (1983) *Methods in Yeast Genetics*. Cold Spring Harbor Laboratory Press, Cold Spring Harbor, NY.
Smith,G.R. (1988) *Microbiol. Rev.*, **52**, 1–28.
Strathern,J.N. (1988) In Kucherlapati,R. and Smith,G.R. (eds), *Genetic Recombination*. American Society for Microbiology, Washington, D.C., pp. 445–464.
Strathern,J.N., Spatola,E., McGill,C. and Hicks,J.B. (1980) *Proc. Natl. Acad. Sci. USA*, **77**, 2839–2843.
Strathern,J.N., Klar,A.J., Hicks,J.B., Abraham,J.A., Ivy,J.M., Nasmyth,K.A. and McGill,C. (1982) *Cell*, **31**, 183–192.
Sugino,A., Nitiss,J. and Resnick,M.A. (1988) *Proc. Natl. Acad. Sci. USA*, **85**, 3683–3687.
Sun,H., Treco,D., Schultes,N.P. and Szostak,J.W. (1989) *Nature*, **338**, 87–90.
Szostak,J.W., Orr-Weaver,T.L., Rothstein,R.J. and Stahl,F.W. (1983) *Cell*, **33**, 25–35.
Tanaka,K., Oshima,T., Araki,H., Harashima,S. and Oshima,Y. (1984) *Mol. Cell. Biol.*, **4**, 203–211.
Weiffenbach,B. and Haber,J.E. (1981) *Mol. Cell. Biol.*, **6**, 522–534.
Weinert,T.A. and Hartwell,L.H. (1988) *Science*, **241**, 317–322.

Received on October 20, 1989